Short communication

Synthesis and characterization of doped Li[Mn$_{0.5-x/2}$Ni$_{0.5-x/2}$Co$_x$]O$_2$ positive electrode materials

Jörg Reim [a,*], Harald Rentsch [a], Werner Scheifele [b], Petr Novák [b]

[a] *Ferro GmbH, Gutleutstrasse 215, D-60327 Frankfurt am Main, Germany*
[b] *Paul Scherrer Institut, Electrochemistry Laboratory, CH-5232 Villigen PSI, Switzerland*

Abstract

Layered positive electrode materials for rechargeable lithium-ion batteries of the general formula Li[Mn$_{0.5-x/2}$Ni$_{0.5-x/2}$Co$_x$]$_{1-y}$M$_y$O$_2$ ($x \leq 1/3$, $0 \leq y \leq 0.05$) were synthesized by a solid state route. The effect of doping elements M on the electrochemical performance was investigated. It was found that doping with niobium or tantalum has a positive effect on the cycling stability compared to the undoped parent compounds ($y = 0$). High discharge capacities, excellent cycling stabilities and high rate capabilities were achieved.
© 2007 Published by Elsevier B.V.

Keywords: Rechargeable battery; Layered oxide

1. Introduction

Layered positive electrode materials based on a Li–Mn–Ni chemistry promise several advantages over the widely used LiCoO$_2$: better electrochemical performance, improved safety and lower cost. In early studies the effect of Mn:Ni ratio and synthesis conditions were investigated on electrochemical performance, but most of the materials lacked practical usefulness [1–3]. In 2001, Novák et al. were successful in stabilizing the oxide by introducing aluminum [4]. Li[Mn$_{0.5}$Ni$_{0.4}$Al$_{0.1}$]O$_2$ showed high capacity and excellent cycling stability even at elevated temperatures. Ohzuku et al. were able to synthesize Li[Mn$_{0.5}$Ni$_{0.5}$]O$_2$ with very good electrochemistry by applying a calcining temperature of 1000 °C [5]. Cobalt containing compounds such as Li[Mn$_{1/3}$Ni$_{1/3}$Co$_{1/3}$]O$_2$ exhibited an even better performance [6]. However, due to the high price of cobalt, a low Co content is critical for industrial application and commercial success.

Therefore, in the present study, we investigated layered positive electrode materials of the general formula Li[Mn$_{0.5-x/2}$ Ni$_{0.5-x/2}$Co$_x$]O$_2$ with $x < 1/3$. The materials were synthesized by a simple and cost-effective production route. We were specifically interested if the expected reduction of electrochemical performance due to lower cobalt content could be counteracted by the introduction of dopants.

In the literature it is reported that the electrochemical performance of positive electrode materials may be improved by doping. The choice and the applicability of the doping element are strongly dependent on the type of positive electrode material, although B, Al and Mg seem to have the broadest applicability [4,7,8]. In a systematic study, we tried to introduce a broader range of dopants with different valence states and varying ionic radii: +2 Mg, +3 B, Al, Y, In, La, +5 Nb and Ta.

2. Experimental

2.1. Synthesis procedure

The lithium complex oxides were synthesized by a solid-state method. Commercial oxides, hydroxides and/or carbonates of the respective elements were used. Lithium carbonate, a nickel compound, a manganese compound, a cobalt compound and a compound of the doping element (boric acid, aluminum hydroxide, gallium oxide, magnesium hydroxide, niobium(V) oxide or tantalum(V) oxide, respectively) were mixed together in the appropriate ratio and fired at 1000 °C for 10 h in air. After cooling, the product was crushed and ball-milled to a powder with a particle size of $d_{90} < 20$ μm. Phase identity and purity of the products was checked using powder XRD.

---

* Corresponding author.

2.2. Analytical methods

Powder X-ray diffraction was carried out on a Philips PW 1800 diffractometer with Cu Kα radiation, operated at 40 kV and 30 mA, with automatic divergence slit and graphite monochromator. Data were collected in the 2θ-range of 5–120° using a step size of 0.02° and a counting time of 1s per step. Qualitative analyses were carried out with the X'Pert HighScore software (Panalytical) using the records from the International Centre for Diffraction Data PDF-2 database. Quantitative analyses were carried out using the Rietveld method implemented in the X'Pert Plus software (Panalytical).

Secondary electron images were obtained with the electron microprobe Jeol JX 8900 RL equipped with a W filament at 15 kV and at beam currents below 10^{-10} A.

2.3. Electrochemical characterization

Test electrodes comprising aluminum foil current collectors were prepared by the standard doctor blade technique starting from N-methylpyrrolidone-based slurries of active material. The composition of the electrodes was as follows: 85.7% of active mass, 4.75% of a polyisobutene binder (Oppanol® B200, BASF AG, Ludwigshafen, Germany) and 9.55%, mixture of carbon black (15% Ensaco® 250, Hubron Ltd., Manchester, England) and graphite (85% TIMREX® MB15, TIMCAL SA, Bodio, Switzerland). The cast slurries were dried at 80 °C under vacuum to evaporate the solvent. The electrode were then punched with a diameter of 13 mm and dried over night at 120 °C under vacuum before use. The active material load was about 10 mg cm^{-2}.

The electrochemical cycling experiments were conducted in two-electrodes, titanium-based cells. All cell parts were dried at 80 °C under vacuum before use.

The oxides were tested against lithium metal as counter electrode. The electrolyte used was battery grade ethylene carbonate and dimethyl carbonate (1:1), with 1 M LiPF$_6$ and was obtained from Ferro Corp. (Independence, OH, USA). The electrochemical measurements were conducted in combined galvanostatic–potentiostatic protocol. First, classical galvanostatic (constant current) cycling with a specific current of 30 mA g^{-1} in the beginning, increasing up to 600 mA g^{-1} during further cycling (cf. Fig. 3) was performed until an upper voltage limit of 4.4 V versus Li/Li$^+$ and a lower voltage limit of 3.0 V versus Li/Li$^+$, respectively, for the charge and discharge. At the end of each charge step a potentiostatic step followed, with a reduction of the current at the fixed upper potential limit down to a value of 3 mA g^{-1}, to complete the charging. The cells were cycled galvanostatically by means of a computer-controlled cell capture system CCCC (Astrol Electronics AG, Oberrohrdorf, Switzerland).

3. Results and discussion

One goal of this work was to establish a simple and cost-effective production route for Li[Mn$_{0.5-x/2}$Ni$_{0.5-x/2}$Co$_x$]O$_2$ type compounds. We chose the composition with $x = 0.1$, LiMn$_{0.45}$Ni$_{0.45}$Co$_{0.1}$O$_2$ (**1**), as the base and reference compound for our studies. We focused on solid-state methods using metal oxides, hydroxides and carbonates as precursor compounds. Materials were chosen that are commercially available in bulk quantities. Single-phase products were obtained after one firing step at 1000 °C. Prerequisite is the proper choice of reactive raw materials in combination with the appropriate mixing technology. In the course of our work, we could show that our method is also applicable to other compositions, namely for $x \leq 1/3$.

In our doping study we tried to introduce 1 or 5 mol% of the selected dopant into our reference composition **1**. This means, we applied our synthesis method to a series of low Co containing compounds Li[Mn$_{0.45}$Ni$_{0.45}$Co$_{0.1}$]$_{1-y}$M$_y$O$_2$ with $y = 0.01$ and 0.05, respectively. In a first step, it was verified by powder XRD if the doping element M was incorporated into the host structure or not. The Rietveld method was used to determine the lattice constants of the target compound and to calculate the phase compositions if more than one phase was present.

Yttrium, indium and lanthanum could not be introduced into the structure. As raw materials, Y$_2$O$_3$, In$_2$O$_3$ and La(OH)$_3$ were used. In case of yttrium, LiYO$_2$ and Y$_2$O$_3$, in case of indium, Li(Ni$_{0.5}$In$_{0.5}$)O$_2$ and in case of lanthanum, La$_2$Li$_{0.5}$Co$_{0.5}$O$_4$ and LaNiO$_3$ were detected as secondary phases in quantitative amounts, respectively. To verify if this is attributed to the reactivity of the raw materials, the experiments were repeated using the corresponding nitrates which should reveal a higher reactivity. But this had no significant effect on the resulting phase compositions. For the case of boron, only the 1% doped material could be synthesized. If higher B doping was tried, XRD revealed Li$_3$BO$_3$ as a secondary phase.

On the other hand, magnesium, aluminum, gallium, niobium and tantalum could be incorporated into the structure up to 5 mol% proved by phase analysis and determination of lattice constants. Table 1 gives an overview of this first series of prepared samples.

We attribute this mainly to size effects. Table 2 lists the effective ionic radii of the relevant elements and oxidation states [9]. All radii refer to a coordination number of six, for Co^{3+} the low-spin state was assumed. Y^{3+}, In^{3+} and La^{3+} ions are too big, while B^{3+} is too small and Mg^{2+}, Ga^{3+}, Nb^{5+} and Ta^{5+} fit perfectly into the transition metal layer.

Table 1

Overview of prepared samples of the doping series Li[Mn$_{0.45}$Ni$_{0.45}$Co$_{0.1}$]$_{1-y}$M$_y$O$_2$ and discharge capacities [mAh g^{-1}] after 4th and 30th cycle (3.0–4.4 V/CCCV/30 mA g^{-1})

Compound	M	y	Discharge capacity 4th cycle [mAh g^{-1}]	Discharge capacity 30th cycle [mAh g^{-1}]
1	–	0	146	137
2	B	0.01	146	140
3a	Al	0.01	147	138
3b	Al	0.05	136	127
4a	Ga	0.01	145	138
4b	Ga	0.05	137	107
5a	Mg	0.01	141	134
5b	Mg	0.05	118	113
6a	Nb	0.01	148	146
6b	Nb	0.05	Not tested	
7a	Ta	0.01	147	143
7b	Ta	0.05	Not tested	

Table 2
Effective ionic radii [9]

Ion	Charge	Ionic radius [Å]
Li	+1	0.76
Mn	+4	0.53
Ni	+2	0.69
Co	+3	0.55
B	+3	0.27
Al	+3	0.55
Ga	+3	0.62
In	+3	0.80
Y	+3	0.90
La	+3	1.03
Nb	+5	0.64
Ta	+5	0.64

Fig. 2. SEM picture of **8**.

Fig. 1 shows the diffraction pattern of compound **8** ($Li[Mn_{0.42}Ni_{0.42}Co_{0.16}]_{0.99}Nb_{0.01}O_2$, see below) as a typical example. The reflections can be indexed in the hexagonal system according to space group R-3 m. Reflections 018 and 110 are clearly split, also indicating the layered nature of the material. This was also confirmed by Rietveld refinements. The reflections show nearly no broadening indicating a high degree of crystallinity.

Scanning electron microscopy was carried out to determine particle sizes and morphology (Fig. 2). Primary particles are mainly between 0.5 and 3 μm, which are somehow agglomerated. This in accordance with particle size measurements by laser granulometry giving typical values of d_{10} of ca. 1 μm, d_{50} of ca. 2–4 μm and d_{90} of ca. 10–15 μm.

Compounds **1**, **2**, **3a**, **3b**, **4a**, **4b**, **5a**, **5b**, **6a** and **7a** were electrochemically tested in half-cells in the voltage range 3.0–4.4 V. Table 1 shows the measured discharge capacities in the 4th and 30th cycle. The undoped material **1** starts at 146 mAh g^{-1} and shows only a moderate cycling stability with a loss of 9 mAh g^{-1} up to the 30th cycle. The 1% doped materials show approximately the same starting values in the 4th cycle. Doping with 1% B shows a slightly positive effect on cycling stability, while doping with 1% Al and Ga show nearly no effect and doping
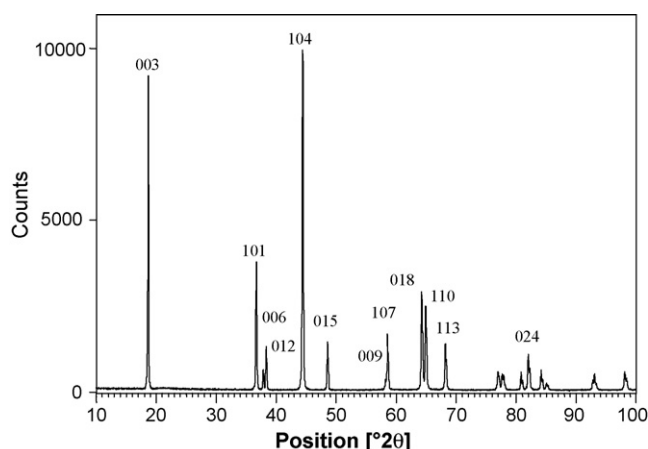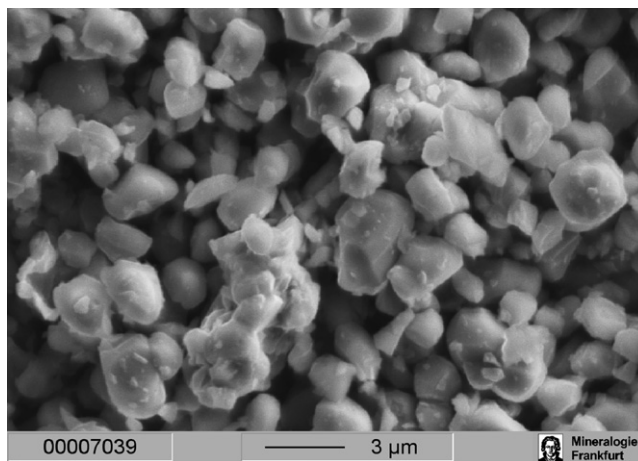
with 1% Mg even shows a negative effect. On the other hand, doping with 1% Nb improves the cycling stability significantly from the 4th to the 30th cycle, only a loss of 2 mAh g^{-1} is observed. The effect of 1% Ta doping is not as high as that of Nb, but the compound still performs better than the comparative examples. Doping with 5% of Al, Ga and Mg deteriorates the electrochemical performance markedly.

In a second step, we optimized our manufacturing procedure and studied higher Co containing compositions. Improvements of synthesis conditions resulted in a significant increase of capacity. For the most promising composition **6a**, a discharge capacity of 158 mAh g^{-1} (4th cycle, rate: 30 mA g^{-1}) was achieved while maintaining the good cycling stability.

Higher Co containing compounds were synthesized, e.g. $Li[Mn_{0.42}Ni_{0.42}Co_{0.16}]_{0.99}Nb_{0.01}O_2$ ($x = 0.16$, $y = 0.01$, M = Nb, **8**) and for comparison, we also synthesized undoped $Li[Mn_{1/3}Ni_{1/3}Co_{1/3}]O_2$ ($x = 1/3$, $y = 0$, **9**) using our solid-state route. Besides capacity and cycling stability, we also studied rate capability from 30 to 600 mA g^{-1}. For compound **8**, a high initial discharge capacity of 162 mAh g^{-1} (30 mA g^{-1}), excellent cycling stability and very good rate capability are observed. As expected, doubling of Co content as in **9** improves the electrochemical performance at high rates. This is illustrated in Fig. 3.
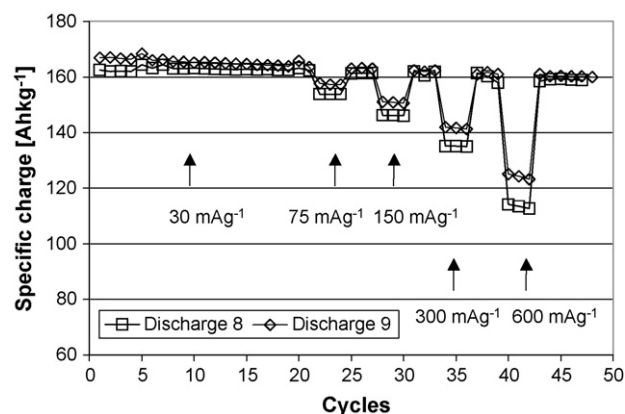

Fig. 1. X-ray diffraction pattern of **8**.

Fig. 3. Cycling behavior and rate capability tests of **8** and **9** (3.0–4.4 V vs. Li/CCCV).

4. Conclusions

Layered positive electrode materials of the general type $Li[Mn_{0.5-x/2}Ni_{0.5-x/2}Co_x]O_2$ with excellent electrochemical performance were prepared by a cost-effective solid state route. They are characterized by high discharge capacities and excellent cycling stabilities. We demonstrated the beneficial effect of introducing Nb and Ta to low Co containing compounds ($x \ll 1/3$).

Acknowledgment

References

[1] E. Rossen, C.D.W. Jones, J.R. Dahn, Solid State Ionics 57 (1992) 311–318.
[2] D. Caurant, N. Baffier, V. Bianchi, G. Grégoire, S. Bach, J. Mater. Chem. 6 (1996) 1149–1155.
[3] M.E. Spahr, P. Novák, B. Schnyder, O. Haas, R. Nesper, J. Electrochem. Soc. 145 (1998) 1113–1121.
[4] P. Novák, R. Nesper, M. Coluccia, F. Joho, A. Piotto Piotto, Abstract No. 56 Lithium Battery Discussion Electrode Materials, Arcachon, France, 2001.
[5] T. Ohzuku, Y. Makimura, Chem. Lett. 30 (2001) 744–745.
[6] T. Ohzuku, Y. Makimura, Chem. Lett. 30 (2001) 642–643.
[7] R. Alcántara, P. Lavela, J.L. Tirado, R. Stoyanova, E. Zhecheva, J. Solid State Chem. 134 (1997) 265–273.
[8] C. Delmas, L. Croguennec, MRS Bull. 27 (2002) 608–612.
[9] R.D. Shannon, Acta Cryst. A32 (1976) 751–767.